Progress In Electromagnetics Research M, Vol. 41, 189–198, 2015

Electromagnetic Waves under Sea: Bow-Tie Antenna Design for Wi-Fi Underwater Communications

Evangelia A. Karagianni*

Abstract—In this paper the propagation of electromagnetic waves in a medium with non zero conductivity is discussed, analyzing the dielectric properties of the sea water, in order to accurately characterize a wireless communication channel. Mathematical models for sea water dielectric constant, wavelength, propagation speed and path loss when an electromagnetic wave at 2.4 GHz propagates through sea water are presented. A Bow-Tie microstrip antenna that is required to overcome the high path loss and bandwidth requirements in sea water is studied. A dual-band antenna, with arc-shaped circular slots, operating for IEEE802.11 b/g/n standards, at 2.4 GHz and 5.1 GHz for WLAN communications, with dimensions 1.4 cm^2 is implemented. Return loss, input impedance and gain have been extracted in order to characterize antennas' performance in a conductive medium.

1. INTRODUCTION

Underwater Wireless Sensor Networks (WSN) are sensors used to monitor environmental or physical phenomena such as temperature, humidity, pressure, vibration, or motion and to cooperatively disseminate the data through the network of sensors to a shore access point [1]. Coastline protection, off-shore oil/gas field monitoring, oceanographic data collection, autonomous or remotely operated underwater vehicles are some of the applications of WSN [2]. As wireless network sensors become smaller in dimensions and cheaper, researchers deploy them in unconventional environments [3]. WSN are stationed underground or underwater, in order to monitor soil or sea properties respectively and then transmit the collected data to an access point on the surface as presented in Figure 1 [5].

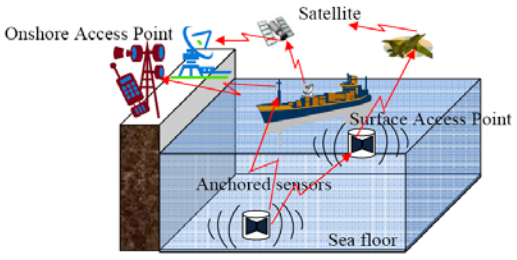

Figure 1. An underwater wireless sensor network.

Due to the high attenuation of the electromagnetic signal in water, most of the underwater wireless sensors rely on sonic transducers for wireless communication employing sound waves, and this is a

Received 21 January 2015, Accepted 19 March 2015, Scheduled 29 March 2015
* Corresponding author: Evangelia A. Karagianni (evka@hna.gr).
The author is with the Electronics Laboratory, Department of Naval Science, Hellenic Naval Academy, Hadjikyriakou Avenue, Piraeus 18539, Greece.

proven technology [7, 8]. Due to the fact that sonic transceivers use many nodes to overcome the high path losses in water, the cost is significantly high. The main advantage of using electromagnetic waves instead of sound waves is that they have faster propagation, resulting in a high data rate due to their high frequency of the wave. As IEEE 802.11 is the current standard for wireless local area networks (WLAN), recently published research projects [4] focus on applications such as warning systems for seismic waves alert or monitoring the sea for pollution.

1.1. Motivation

The motivation for this research is the high design and maintenance costs of acoustic and optical systems. WLAN, also referred as Wi-Fi, has the potential to provide an ideal solution for certain applications, where high data rate transmission is required at short distances. Because WLAN devices are globally available, their cost is relatively low, and there is adequate knowledge in handling them. The use of frequencies that are part of the unlicensed ISM (Industrial, Scientific and Medicine) radio bands does not bear any cost for the user, also contributes to the low cost for the WLAN. Beside the main purpose of ISM bands, there has been rapid growth in their use in low-power and short-range communications.

1.2. Recently Published Research Methods

Today, research on underwater communications focuses on increasing the distance between the communicating points, to create more broadband networks as well as to reduce energy consumption with a significant effect on the network lifetime [1, 3]. Underwater propagation relies on optical, electromagnetic, acoustic or ultrasonic signals and ongoing research methods based on these techniques have advantages and drawbacks, as summarized bellow [5].

Optical signals can reach very high propagation speeds. However, the particles present in the sea water (salinity and turbidity) causes scattering signals, so optical systems seem not to be the best option for long distances [6]. Systems based on acoustic signals are less susceptible to sea particles than the optical ones. Since they are able to reach distances over 20 km [7], they are used widely. Underwater communication based on acoustic signals presents some disadvantages, such as the low data rate, up to 30 kbps, the dependence of the salinity and the low frequency. Even more, when the communication is performed near the surface, the attenuation is stronger due to the multiple reflections.

Electromagnetic signals have higher data rates, up to 10 Mbps, but for very short distances. The speed of EM waves is higher than that of acoustic ones and mainly depends on permeability (μ), permittivity (ε), conductivity (σ) and volume charge density (ρ) [8]. These parameters change with the type of water, thus the wave propagation speed also varies. Taking into consideration that the dielectric constant of seawater varied with variations in frequency, the temperature and the salinity of the sea water [9, 10], the main problem with underwater communications using electromagnetic waves is the high attenuation due to the water conductivity. This attenuation increases with the increasing of the frequency.

2. PRINTED PLANAR ANTENNAS FOR WIRELESS COMMUNICATION

Microstrip antennas are suitable for many mobile applications such as handheld devices, aircrafts, satellites and missiles. They have mechanical robustness, low manufacturing costs, compatibility with MMIC (Monolithic Microwave Integrated Circuits) designs and they are relatively light, tunable and compact. Some of the limitations of the microstrip antennas are relatively low efficiency due to dielectric and conductor losses, low power, spurious feed radiation and narrow bandwidth. These antennas are applicable in the GHz range. For lower frequencies, their dimensions become too large.

Generally, a microstrip antenna consists of thin metallic patches of various shapes etched on dielectric substrates of thickness h, as presented in Figure 2, which usually varies from $0.003 \cdot \lambda_0$ to $0.05 \cdot \lambda_0$, where $\lambda_0 = c/f$. For the purposes of this paper, where $f = 2.4$ GHz, these values are between 0.4 mm to 6 mm. The substrate is grounded at the opposite side. The dimensions of the patch are usually within the range $0.2 \cdot \lambda_0$ to $0.5 \cdot \lambda_0$, in our case between 25 to 62 mm. The dielectric constant (ε_r) of the substrate is usually in the range from 2.1 (Polyflon CuFlon) to 12 (silicon). The most common designs use relatively thick substrates with lower ε_r because they provide better efficiency and

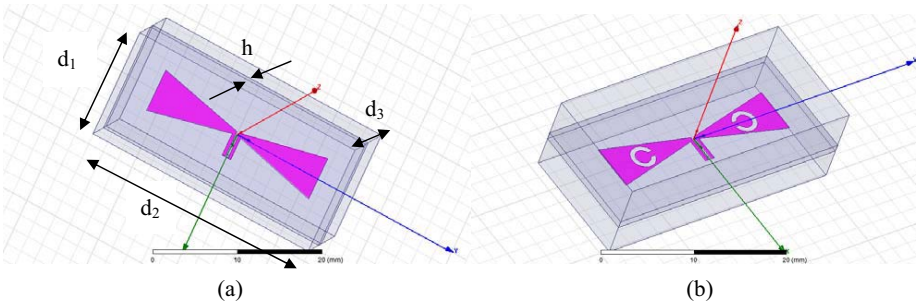

Figure 2. (a) The microstrip Bow-Tie antenna on duroid dielectric $h = 1$ mm operating at 2.4 GHz. (b) The proposed Bow-Tie antenna with circular slots resonating at 2.4 GHz and 5.1 GHz bands for IEEE 802.11 standard.

wider bandwidth. On the other hand, this implies larger dimensions of the antennas. The choice of the substrate is limited by the RF or microwave circuit coupled to the antenna, which has to be built on the same board.

The types of microstrip radiators are single radiating patches such as square, rectangular, bipole, circular, elliptical, triangular, disc sector, circular ring or single slot radiator, or microstrip traveling wave antennas, or Microstrip antenna arrays [11–15]. A self-complementary shaped multiple L-slot loaded suspended microstrip patch antenna is presented in [11] with gain around 8 dBi for 2.4/5.2 GHz band WLAN and 2.5/3.3/5.8 GHz band WiMAX networks. Enhanced bandwidth is achieved in [12] using parasitic elements, at a maximum of 33%, operating over frequency ranges from 2400–2500 MHz and 4900–5875 MHz, for an acceptable VSWR ratio of 2 : 1. In [13], an antenna with frequency band of 3.6 to 10.8 GHz is proposed, having an area reduction of 15% and offering an impedance bandwidth as high as 100% at a centre frequency of 7.2 GHz for $S_{11} < -10$ dB.

The proposed Bow-Tie antenna, as illustrated in Figure 2, is made from a bi-triangular sheet of Duroid substrate. Bow-tie antennas, which are very attractive mainly due to their simplicity and wideband property, are actually a flat version of bi-conical bipole antenna [16]. These antennas have many advantages such as low fabrication cost, high radiation efficiency, ease of manufacturing and low profile [17]. The first step for designing an antenna is to choose proper dimensions for the bow tie arms. Then, select the substrate's thickness and matching feed lines. The feeding of such a structure is done by designing two parallel strip lines connected to a wave port which is placed on one side of the substrate. The proposed antenna can operate for IEEE802.11, b, g, n standards at 2.4 GHz and 5.1 GHz.

Surface waves can be excited at the dielectric-to-water interface. The phase velocity of the surface waves is strongly dependent on the dielectric constant ε_r and thickness h of the substrate (see Figure 2). The excitation of surface waves in a dielectric slab backed by a ground plane has been well studied for dielectric-to-air interfaces. The cut-off frequencies for the higher-order modes (TM_m and TE_m) are given by:

$$f_c^{(m)} = \frac{m \cdot v}{4 \cdot h \cdot \sqrt{\chi_e}}, \quad m = 1, 2, \ldots \tag{1}$$

where h is the substrate thickness, χ_e the electric susceptibility of a medium given in Equation (8), and v the speed of light underwater $v = \frac{1}{\sqrt{\mu \cdot \varepsilon}} = \frac{c}{n} = \frac{c}{\sqrt{\mu_r \cdot \varepsilon_r}}$, where c is the speed of light in vacuum, n the refractive coefficient of the medium, μ the absolute permeability ($\mu = \mu_0 \cdot \mu_r$), μ_r the relative permeability, ε the absolute permittivity, ε_r the relative permittivity or dielectric constant of the medium, and μ_0 and ε_0 are vacuum's absolute permeability and permittivity, respectively ($\varepsilon_0 = 8.85 \times 10^{-12}$ F/m, $\mu_0 = 4\pi \times 10^{-7}$ H·m^{-1}).

The cut-off frequencies for TE_m modes are given by the odd m, and the cut-off frequencies for TM_m modes are given by the even m. For TE_1 mode, the calculated values of h/λ_c are 0.23 for duroid ($\varepsilon_r = 2.2$) and 0.08 for alumina ($\varepsilon_r = 10$).

The substrate thickness is chosen so that the ratio h/λ_0 is quite below h/λ_c

$$h < \frac{v}{4 \cdot f_h \cdot \sqrt{\chi_e}} \tag{2}$$

where f_h is the upper frequency in the band of interest. In our case, we will use duroid, and the upper frequency is 6 GHz, so the height of the substrate has to be less than 1.3 mm, compared with the value 11.4 mm which is the maximum height of the substrate when the antenna works in vacuum.

3. SEA WATER PROPERTIES

The propagation of EM waves in sea water is significantly different from that on air because seawater has distinct electrical properties that severely impact the signal propagation. The time-harmonic version of Maxwell's equations states that

$$\nabla \times H = \overline{J} + \left(\sigma_e + j \cdot \omega \cdot \varepsilon'\right) \cdot E = J_i + j \cdot \omega \cdot \varepsilon' \left(1 - j \cdot \tan \delta_e\right) \cdot E \tag{3}$$

where E and H are the electric and magnetic field strength respectively. J_i is the impressed electric current density, an excitation to the system by an outside source, σ_e the effective conductivity, and $\tan \delta_e$ the effective loss tangent, both given as:

$$\sigma_e = \sigma_s + \omega \cdot \varepsilon'' \tag{4}$$

$$\tan \delta_e = \frac{\varepsilon''}{\varepsilon'} + \frac{\sigma_s}{\omega \cdot \varepsilon'} \tag{5}$$

where σ_s is the static conductivity and $\omega\varepsilon$ the conductivity due to the alternating field.

The dependence of the dielectric constant ε_r is as appeared in Equation (3), and the effective loss tangent on frequency is referred to as frequency dispersion.

3.1. Conductivity

The conductivity (σ) of a medium affects the transmission of an EM wave through that medium. Specifically, the transmitted signal will face more attenuation as the conductivity of the medium increases. For example, sea water has a high conductivity average value, which changes with the salinity and physical properties of each kind of sea water and is stated to be around 4 S/m [5, 9]. For pure water the typical value ranges [8] between 0.005 and 0.01 S/m.

The conductivity of sea water in relation to temperature (T) and salinity (S) has been measured in laboratory experiments [18]. In a salinity range 20 ppt $< S <$ 40 ppt, the relation is

$$\sigma = \sigma_0 \cdot S \cdot \frac{37.5 + 5.4 \cdot S + 0.015 \cdot S^2}{1004.8 + 182.3 \cdot S + S^2} \cdot \left(1 + \frac{\frac{6.9+3.3 \cdot S - 0.1 \cdot S^2}{84.6+69 \cdot S+S^2} \cdot (T - 15)}{49.8 - 0.23 \cdot S + 0.2 \cdot S^2 + T}\right) \tag{6}$$

where T is in degrees centigrade, s in parts per thousand, σ in siemens per meter. σ_0 is the conductivity at $S = 35$ ppt and is given in dependance of temperature

$$\sigma_0 = 2.9 + 8.6 \cdot 10^{-2} \cdot T + 4.7 \cdot 10^{-4} \cdot T^2 - 3 \cdot 10^{-6} \cdot T^3 + 4.3 \cdot 10^{-9} \cdot T^4 \tag{7}$$

Using Equations (9) and (10), it is calculated that $\sigma_0 = 5.3$ S/m for salinity 35 ppt and 25°C temperature In this paper, salinity is assumed to be a constant value of 38 ppt, which is the average value measured in Mediterranean Sea. The conductivity value which responds to 38 ppt salinity and 25°C temperature is set to be $\sigma = 5.6$ S/m.

3.2. Relative Permeability and Permittivity

Permeability (μ) is the ability of the medium to store magnetic energy. Since seawater is a nonmagnetic medium, it has the same permeability as vacuum [8].

The relative permittivity (ε_r), also known as the dielectric constant, describes the ability of a medium to transmit an electric field. The relative permittivity of seawater is usually set to 81 [5]. But, in general, it is a complex value and depends on other factors such as the salinity of seawater, the temperature and the propagating frequency as well. The mean value of the dielectric constant of sea water for 25°C was experimentally extracted [18, 19]:

$$\varepsilon(\omega) = \varepsilon_0 \cdot \varepsilon_r(\omega) = \varepsilon' - j \cdot \varepsilon'' = \varepsilon_0 \cdot (1 + \chi_e) = \varepsilon' \cdot (1 - j \cdot \tan \delta_e) \tag{8}$$

$$\varepsilon_r(\omega) = \left(\varepsilon_\infty + \frac{\varepsilon_s - \varepsilon_\infty - \varepsilon_{salt}}{1 + (\omega \cdot \tau)^2}\right) - j \cdot \left(\frac{\sigma}{\omega \cdot \varepsilon_0} + \frac{\omega \cdot \tau \cdot (\varepsilon_s - \varepsilon_\infty - \varepsilon_{salt})}{1 + (\omega \cdot \tau)^2}\right) \tag{9}$$

where $\omega = 2\pi f$ is the angular frequency, and ε_s and ε_∞ are the real relative permittivity at low and high frequencies, respectively given as $\varepsilon_s = 81$, $\varepsilon_\infty = 4.5$. τ is the relaxation time, the delay of the particles to respond to the field change. For water at 25°C the relaxation time is 8.27 ps, σ the conductivity of water ($\sigma = 4$), ε_{salt} a correction parameter depending on water concentration in salt and the average hydration number of the individual ions which is assumed negligible.

Considering $\omega\tau = 1/8$ which corresponds to 2.4 GHz frequency, we obtain the real part of the relative permittivity as 79.8, and it is independent of conductivity. The imaginary part consists of two components. The first one is obtained to be 41.9 for $\sigma = 5.6\,\mathrm{S/m}$ and $f = 2.4\,\mathrm{GHz}$, while the second one equals 9.625.

Within the frequency range used, we assume that the real part of the dielectric is constant, approximately equal to 80 (which is very close to the practical extracted value 77 [18]), and the imaginary part is equal to 9.6 (close to the practically extracted value 9.3), for 2.4 GHz frequency. This is in accordance with the calculated value of 9.625 if we ignore the ε dependence from the conductivity.

3.3. Intrinsic Impedance of the Sea Water

The intrinsic impedance is a medium property that describes the ratio of the electric field strength to the magnetic field strength [9], and this is the wave impedance of the electromagnetic wave when propagates through it. The intrinsic impedance of the air has been calculated to $Z_0 = 377\,\Omega$. However, the intrinsic impedance of sea water is a complex value and is expressed as a function of permeability (μ), permittivity (ε), conductivity (σ), and angular frequency ($\omega = 2\pi f$).

$$Z = \sqrt{\frac{j \cdot \omega \cdot \mu}{\sigma + j \cdot \omega \cdot \varepsilon}} \tag{10}$$

In case that we ignore the medium conductivity, the wave impedance for sea water environment as a non-magnetic environment is $Z = \frac{377}{\sqrt{\varepsilon_r}} = 42\,\Omega$.

3.4. Underwater Path Loss

For proper deployment of any wireless communication system, it is critical to have accurate channel characterization. Path loss represents the difference between the transmitted signal power and received signal power. Received power as a function of transmitted signal P_t, underwater path loss L and gains of the receiver G_r and transmitter G_t antenna can be described by the following:

$$P_r = P_t + G_t + G_r - L \tag{11}$$

Free Space Path Loss is

$$L_{\mathrm{FreeSpace}} = 20 \cdot \log\left(\frac{4 \cdot \pi \cdot d}{\lambda_0}\right) \mathrm{dB} \tag{12}$$

where d is the distance between the transmitter and the receiver in meters and λ_0 the wavelength in free space measured in meters too.

In order to realize the impact of the complex permittivity on the attenuation factor, the attenuation loss is derived from the propagation constant γ, which is expressed (using Equations (3) and (10)) as

$$\gamma = \alpha + j \cdot \beta = \omega \cdot \sqrt{\mu \cdot \varepsilon - j \cdot \frac{\sigma \cdot \mu}{\omega}} = \omega \cdot \sqrt{\frac{\mu \cdot \varepsilon' \cdot (1 - \cos\delta_e)}{2 \cdot \cos\delta_e}} + j \cdot \omega \cdot \sqrt{\frac{\mu \cdot \varepsilon' \cdot (1 + \cos\delta_e)}{2 \cdot \cos\delta_e}} \tag{13}$$

Taking the real part of the propagation constant α, we obtain the attenuation loss (in dB) in seawater due to seawater conductivity and complex permittivity, as:

$$L = 20 \cdot \log\left(e^{\alpha d}\right) \approx 8.7 \cdot \alpha \cdot d \tag{14}$$

where d is the distance between the transmitting and the receiving nodes.

It is clear that the attenuation loss is very high, and this is due to very high conductivity of seawater, which severely attenuates the propagating EM wave. Such a property sets a tight constraint on the separation distance between the nodes. Also, it is evident that the complex permittivity has a direct impact on the signal attenuation in seawater.

3.5. The Speed of EM Wave Underwater

The communication link is a direct link between the sensor node underwater and the buoy node at the surface. In case that there is a relay (i.e., intermediate node) in between, careful changes must be made. The signal attenuation at the sea water-air boundary is very high. The reflection loss decreases dramatically as the frequency increases from 100 kHz to 1 GHz, and then it remains almost constant (at 4 dBs) for frequencies higher than 2 GHz. The speed of the electromagnetic wave underwater is

$$v_{RF} = \sqrt{\frac{2 \cdot \omega}{\mu \cdot \sigma}} \tag{15}$$

The speed of the EM wave when it propagates in sea water is derived by the simplified equation given in Equation (22). For 2.4 GHz, for $\sigma = 5.3$ S/m this value is approximately 67.3×10^6 m/s. But this speed is limited by the speed of light underwater which is 33.3×10^6 m/s given in Equation (2).

After calculations, another simplified, useful expression for the sea water attenuation is derived [21], which is more accurate for lower than 2 GHz frequencies:

$$L_{sea} \approx \sqrt{\pi \cdot f \cdot \mu \cdot \sigma} \tag{16}$$

4. ANTENNA'S ANALYSIS

Signal reflection due to impedance mismatch has a major impact on the EM wave propagation. Impedance matching is very important in order to maximize the power transfer [3, 8, 18]. For this reason, the feed gap has been studied thoroughly for the Bow-Tie antenna design. It is observed that the high conductivity of sea water drastically increases the path loss and decreases speed. In order to simulate the 3-D full wave electromagnetic fields, ANSYS High Frequency Simulation Software (HFSS) in driven modal solution type is used.

The substrate with height $h = 1$ mm is of duroid dielectric material. A finite conductivity boundary to the copper cladding is assigned. Regarding the excitation, a lumped port with a 50 Ω resistance is used. All analysis is performed firstly in the frequency range 1 GHz to 10 GHz. Therefore, the minimum distance between the water volume wall and the radiating aperture is set to be one quarter wavelength, which means 3.4 mm at 2.4 GHz in sea water, compared to 31 mm in air. So, the volume in Figure 2 has dimensions $d_1 = 14$ mm, $d_2 = 30$ mm, $d_3 = 10$ mm. This water volume is assigned as the radiation boundary.

Finally, far-field setup is inserted with infinite sphere, $-90° < \varphi < 90°$ and $0° < \theta < 360°$. The flare angle of the designed antenna is 28.4°, kept constant for all trials. Parameters optimized in order to have the best results for under-sea propagation were the arm length (characterized by b_1, b_2 and c_1), and matching lines (a_1, a_2) as they are presented in Figure 3.

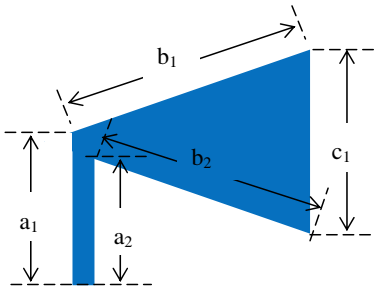

Figure 3. The dimensions of the simulated antenna that presented in Figure 2. $a_1 = 3.5$, $a_2 = 3$, $b_1 = 11.38$, $b_2 = 11.01$, $c_1 = 5.6$. All dimensions are in millimeters.

5. DISCUSSION

The main goal of this research is to design low cost, low profile and easily reproducible antennas. These antennas were designed for the use of WLAN 802.11, b/g/n. For this purpose, we identified four main

objectives. The antenna must have a gain more than 1 dBi, low build cost, small and light weight structure and easy manufacture.

The first antenna, without slots on arms, has a VSWR value approximately 1.2 : 1 at 2.4 GHz — or $S_{11} = -9.9077$ dB as depicted in Figure 4(a) — carrier frequency when working in sea water. The real part of the input impedance is 27 Ω — Figure 4(b) — in sea water, and the maximum gain at $\theta = 0°$ is 1.7 dBi, as shown in Figure 4(c). When working in pure water environment, the antenna resonates at 2.4 GHz with input reflection coefficient −15 dB and a bandwidth of twenty percent, as shown in Figure 4(a). The real part of the input impedance is 33 Ω, and the maximum gain at $\theta = 0°$ is 2.5 dBi. For both cases the imaginary part of the input impedance is very small, between 6 and 10 Ohms. This antenna would not work in air for 2.4 GHz as shown in Figure 5 — green line but at 7.6 GHz has its best performance with −32 dB reflection coefficient.

The second antenna with arc-shaped circular slots, symmetrical on both arms, resonates at two frequencies, 2.4 and 5.1 GHz with excellent simulation performance in sea water as shown Figure 6(a). It has an input reflection coefficient less than −10 dB within frequency ranges (1.88 GHz, 2.56 GHz) and (4.66 GHz, 6.15 GHz). Slots had no effect on the value of the real part of the input impedance as depicted in Figure 6(b). The maximum gain at $\theta = 0°$ is 1.7 dBi — Figure 6(c). When working in pure water reflection reaches −50 dB at 2.15 GHz, having approximately the same bandwidth of about thirty percent. In pure water, for both frequencies the real part of the input impedance is 39 Ω. As stated for the first antenna, this antenna would not work for 802.11 in air environment too. But at 8 GHz the reflection reaches −25 dB with fifteen percent bandwidth.

The experiment was performed in a pool with sea water with 3.1% salinity, for the second designed antenna. A prefabricated remote controlled vehicle, the hydrobot, as shown in Figure 7, has been used [hydrobots.gr]. A network device server certified with a less than 5 dBi gain antenna for wireless 802.11b/g was used. We placed this system inside a sealed waterproof plastic box at the bottom side of the hydrobot. This was used as ballast too in order to immerse the hydrobot and maintain the upright position when the device was submerged.

Tests were performed in deep depth, more than 30 cm. Measurements taken were valid; the signal did not spread out of the water nor was any signal received from air [19]. The system was located at a rational distance (more than 50 cm) from the edge and bottom walls to avoid reflections' effects [20].

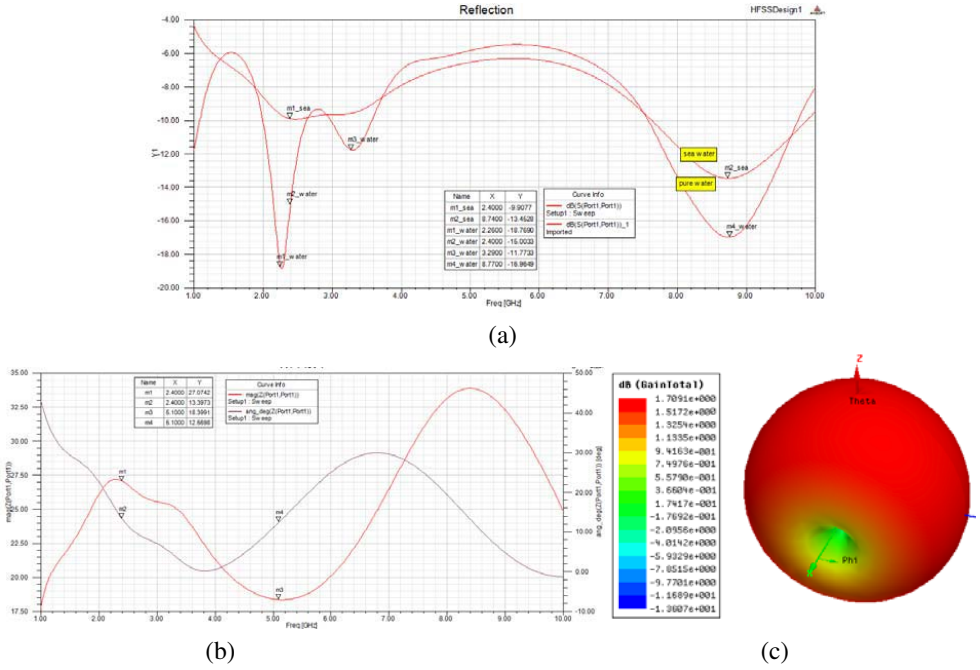

Figure 4. Results for the first design under sea (without slots). (a) Reflection coefficient S_{11} at the input port, in sea water and pure water environment. (b) Input impedance. (c) Gain.

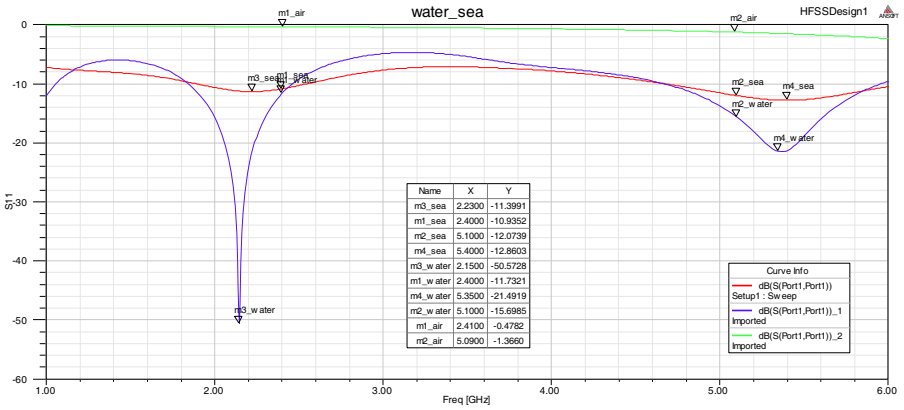

Figure 5. The reflection coefficient S_{11} at the input port for the second proposed antenna with slots for different environments. (a) Sea water, $m1$, $m2$, $m3$, $m4$_sea. (b) Pure water, $m1$, $m2$, $m3$, $m4$_water. (d) Air, $m1$, $m2$_air for the frequency range 1 GHz–6 GHz.

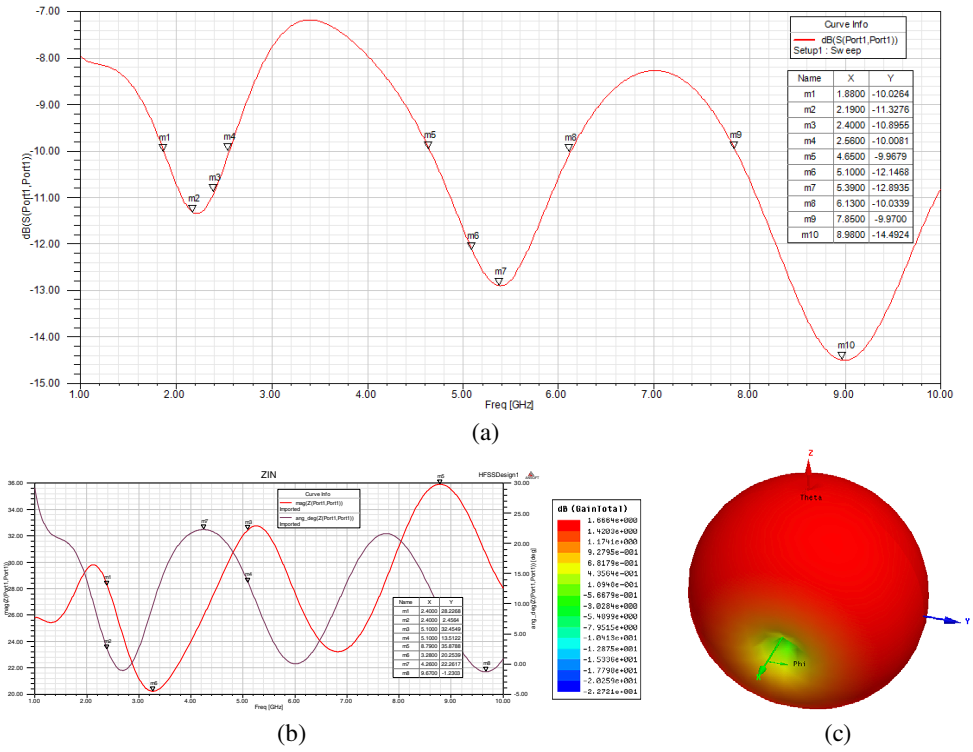

Figure 6. Results for the second design (with slots), in the frequency range 1 GHz–10 GHz, in sea water environment. (a) Reflection coefficient S_{11} at the input port. (b) Input impedance. (c) Gain.

Both sensors had identical features. Antennas were oriented to the bottom, at the two lower tubes in fixed structure, in a constant distance of 15.2 cm between them, with their radiation pattern to down.

This dual-band antenna can work in pure water too, but not in air environment for 802.11 prototypes.

Measurements showed that simulation results almost coincided with the test results. The results, more than expected, satisfied our goals, although the distance was predetermined and constant. Power measures gave −60 dBm in pure water but in sea water with 3.1% salinity, power measured in between −64 dBm to −71 dBm. This proves that the signal although unstable — because of the conductive

Figure 7. The hydrobot used for performing tests. Identical antennas were placed at the lower tubes.

medium — has a satisfactory communication link when the communication link is in sea water. The proposed Bow-Tie antenna has an input reflection coefficient of −12 dB and −16 dB at 2.4 and 5.1 GHz, respectively, and a maximum gain of 1.2 dBi.

6. CONCLUSIONS

In this paper, we discuss the propagation of electromagnetic waves in sea water analyzing the propagation speed and the attenuation in a medium with non-zero conductivity, in order to accurately characterize a wireless propagation medium. Wavelength and path loss are discussed in terms of EM propagation.

The steps that can permit a Bow-Tie antenna to work in sea water with matching feed lines have been presented from design to measurements. Preliminary calculations have been carried out to support the use of the designed Bow-Tie in a two-way communication sensor system. The distance between access points is 15.2 cm and kept constant. The flare angle of the proposed antenna is 28.4° and kept constant too. The arm length and matching lines are optimized in order to have the best results for undersea propagation. The extracted dual-band antenna, working for 802.11 b/g/n, has good performance at 2.4 GHz and 5.1 GHz with maximum gain 1.2 dBi at $\theta = 0°$ and a variable received power at −71 to −64 dBm, tested in salty water. Its performance is checked in other mediums such as pure water and air. The radio link attenuation in sea water is 20% higher than that measured in pure water (−60 dBm) when the link distance is constant, and it is only −30 dBm when the communication link is air.

The proposed system provides several benefits. On one hand, it is cheap, and on the other hand, it provides high data transfer rates for all types of data, including images. Because the proposed antennas can be used in any depth, they can be used in military or marine applications, although they can be used for very short distances. A sensor that monitors the condition of the hull of a ship can send images to determine the fouling that increases the ship's resistance and thus decide the time that the ship has to be dry-docked or cleaned; it will be particularly useful for ship owners.

Because the temperature of the water affects the conductivity values, refractivity values and consequently the distance, more performance tests will be carried out in future antenna designs to be adapted to the Aegean Archipelagos case. For this reason, future work will estimate the temperature and salinity per season in the area of northwest Aegean Archipelagos and draw a new empirical relationship for conductivity.

REFERENCES

1. Dargie, W. and C. Poellabauer, *Fundamentals of Wireless Sensor Networks: Theory and Practice*, John Wiley and Sons, 2010.
2. Jiang, S. and S. Georgakopoulos, "Electromagnetic wave propagation into fresh water," *Journal of Electromagnetic Analysis and Applications*, Vol. 3, 261–266, 2011.
3. Hunt, K., J. Niemeier, and A. Kruger, "RF communications in underwater wireless sensor networks," *IEEE International Conference on Electro/Information Technology (EIT)*, 2010.

4. Kulhandjian, H., L. C. Kuo, T. Melodia, and D. A. Pados, "Towards experimental evaluation of software-defined underwater networked systems," *Proc. of IEEE Underwater Communications Conf. and Workshop (UComms)*, Sestri Levante, Italy, 2012.
5. Stuntebeck, E., D. Pompili, and T. Melodia, "Wireless under-ground sensor networks using commodity terrestrial motes," *2nd IEEE Workshop on Wireless Mesh Networks*, 2006.
6. Nistazakis, H. E., G. S. Tombras, A. D. Tsigopoulos, E. A. Karagianni, and M. E. Fafalios, "Average and outage capacity estimation of optical wireless communication systems over weak turbulence channels," *Mosharaka International Conference on Communications, Propagation and Electronics, MIC-CPE*, 2009.
7. Liu, L., S. Zhou, and J. Cui, "Prospects and problems of wireless communication for underwater sensor networks," *Wireless Communication & Mobile Computing*, Vol. 8, No. 8, 977–994, Oct. 2008.
8. Che, X., I. Wells, P. Kear, G. Dickers, X. Gong, and M. Rhodes, "A static multi-hop underwater wireless sensor network using RF electromagnetic communications," *29th IEEE International Conference on Distributed Computing Systems*, Canada, 2009.
9. Rhodes, M., "Electromagnetic propagation in seawater and its value in military systems," *SEAS DTC Technical Conference*, Edinburg, UK, 2007.
10. Singh, K., Y. Kumar, and S. Singh, "A modified bow tie antenna with U-shape slot for wireless applications," *International Journal of Emerging Technology and Advanced Engineering*, Vol. 2, No. 10, Oct. 2012.
11. Yurduseven, O., D. Smith, N. Pearsall, and I. Forbes, "A solar cell stacked slot-loaded suspended microstrip patch antenna with multiband resonance characteristics for WLAN and WMAX systems," *Progress In Electromagnetics Research*, Vol. 142, 321–332, 2013.
12. Tze-Meng, O. and T. K. Geok, "A dual-band omni-directional microstrip antenna," *Progress In Electromagnetics Research*, Vol. 106, 363–376, 2010.
13. Zaker, R., C. Ghobadi, and J. Nourinia, "A modified microstrip-fed two-step tapered monopole antenna for UWB and WLAN applications," *Progress In Electromagnetics Research*, Vol. 77, 137–148, 2007.
14. Tawk, Y., K. Y. Kabalan, A. EL-Hajj, C. G. Christodoulu, and J. Costantine, "A simple multiband printed bow tie antenna," *IEEE Antennas and Wireless Propagation Letters*, Vol. 7, 2008.
15. Balanis, C. A., *Antenna Theory Analysis and Design*, 2nd edition, John Wiley and Sons, New York, 2007.
16. Sadek, S. and Z. Katbay, "Ultra wideband CPW bow-tie antenna," *International Conference on Electromagnetics in Advanced Applications, 2009, ICEAA'09*, 261–263, Sep. 14–18, 2009.
17. Marantis, L. and P. Brennan, "A CPW-fed bow-tie slot antenna with tuning stub," *Antennas & Propagation Conference*, Loughborough, UK, Mar. 17–18, 2008.
18. Meissner, T. and F. J. Wentz, "The complex dielectric constant of pure and sea water from microwave satellite observations," *IEEE Transactions on Geoscience and remote Sensing*, Vol. 42, No. 9, Sep. 2004.
19. Hattab, G., M. El-Tarhuni, M. Al-Ali, T. Joudeh, and N. Qaddoumi, "An underwater wireless sensor network with realistic radio frequency path loss model," *International Journal of Distributed Sensor Networks*, 2013.
20. Ulaby, F., R. Moore, and A. Fung, *Microwave Remote Sensing: Radar Remote Sensing and Surface Scattering and Emission Theory, Remote Sensing*, Addison-Wesley, USA, 1981.
21. Balanis, C. A., *Advanced Engineering Electromagnetics*, 2nd edition, John Wiley & Sons, New York, 2012.